The Stability and Nonlinear Evolution of Edge Waves

Jianke Yang

1 Introduction

The classical linear water-wave problem on a wedge-shaped beach can be formulated in terms of a velocity potential ϕ, which satisfies the Laplace equation, a free surface boundary condition, and a sea-bed condition, namely

$$\triangle\phi = 0, \tag{1.1}$$

$$g\phi_y + \phi_{tt} = 0, \quad y = 0, \tag{1.2}$$

$$\phi_y = \phi_x \tan\alpha, \quad y = x \tan\alpha, \tag{1.3}$$

where x is out to sea, y is vertical, z is along the beach, and α is the angle of the beach. Stokes (1846) first noted a solution of these equations that represents edge waves, which are propagating along the beach with their crests perpendicular to the shoreline and have an amplitude that decays exponentially off the coast. This solution for the velocity potential ϕ is

$$\phi = \frac{ga}{\omega} e^{-kx \cos\alpha + ky \sin\alpha} \sin(kz - \omega t), \tag{1.4}$$

where a is the amplitude of the edge wave, and k and ω are the wavenumber and frequency. The dispersion relation between ω and k is

$$\omega^2 = gk \sin\alpha. \tag{1.5}$$

Ursell (1952) further discovered that the Stokes solution is only one of many possible edge-wave modes and that successively more possible modes arise as α decreases. A second one is possible for $\alpha < \frac{1}{6}\pi$, a third for $\alpha < \frac{1}{10}\pi$ and so on. The nth mode appears as α drops below $\frac{\pi}{2(2n+1)}$ and its dispersion relation is

$$\omega^2 = gk \sin(2n+1)\alpha. \tag{1.6}$$

There is also a continuous spectrum of solutions with $\omega^2 > gk$ to complete the representation of general disturbances.

Edge waves are very distinctive on a beach because their maximum amplitudes are on the shoreline. It is now believed that they are responsible for the formation of beach cusps (Guza & Inman 1975) and the generation of rip currents and periodic circulation cells in the nearshore region (Bowen & Inman 1969).

The generation of edge waves has been intensively studied, both experimentally and theoretically, in the last forty years. Greenspan (1956) first demonstrated that large-scale edge waves can be excited by atmospheric forcing due to storms moving along the coastline. For smaller-scale edge waves, in an attempt to explain the experimental observations of Galvin (1965) and Bowen & Inman (1969), Guza & Davis (1974) proposed the nonlinear interaction mechanism of edge waves with incoming wavetrains. Using the shallow-water approximation, they showed that a monochromatic harmonic wavetrain of frequency ω, normally incident and strongly reflected on a beach, is unstable to subharmonic standing edge-wave perturbations of frequency $\frac{1}{2}\omega$. Guza & Inman (1975)'s experiments on a bounded beach indicated that this subharmonic resonance was the strongest, and a subharnomic standing edge-wave was preferentially excited. A synchronous edge wave (same period as the incident wave) was sometimes also excited, but the generation was a higher-order, weaker resonance, and was evident only when the subharmonic resonance was excluded by the beach geometry. If the edge-wave coastline antinode number was low, edge waves would reach a steady state. More interesting was the fact that if the wavenumber was high, the number of edge-wave antinodes sometimes alternated between adjacent integers. In a further development of the theory, Whitham (1976) calculated the leading-order nonlinear corrections to the linear dispersion relation of travelling Stokes edge waves and thus deduced that propagating finite-amplitude edge waves are always unstable to large-scale modulations. Later, Minzoni & Whitham (1977) studied the excitation of standing subharmonic edge waves by a normally incident, strongly reflected wavetrain. They formulated the problem in the full water-wave theory without making the shallow-water approximation and solved it for beach angles $\alpha = \pi/2N$, where N is an integer. Their work confirms the results from the shallow-water theory in the small-beach-angle limit. Akylas (1983) studied the large-scale temporal and spatial modulations of subharmonic edge waves excited by resonant interactions with normally incident, strongly reflected wavetrains, and derived equations governing the modulations of edge-wave envelopes. He then re-examined the modulational stability of a propagating edge-wave train and confirmed that the instability, predicted by Whitham (1976), indeed leads to a series of envelope solitons. He also found that the steady state standing subharmonic edge wave with the wavenumber at exact subharmonic resonance is unstable to large-scale modulations.

Although much work has been done as mentioned above, some important questions remain open. Firstly, the effect of the beach geometry on edge waves has not been analytically studied. All the previous analytical work was done on an open beach. But if the beach is bounded by two sidewalls, which is always the case in experiments, this beach geometry will affect the edge-wave dynamics, sometimes even exclude the excitation of edge waves. This effect shows clearly in Guza & Inman (1975)'s experiments. Secondly, the nonlinear evolution of subharmonic edge waves on a wide beach is still not clear. Since in this situation the spatial large-scale modulation arises as well as the temporal one, the evolution equations of these modulations have been derived by Akylas (1983). But what these equations imply about the edge-wave evolution is not known. One steady state standing subharmonic edge wave was found by Akylas (1983) to be unstable to large-scale modulations. The significance of this finding is not clear. It is worth noting here that the relevant experiments conducted by Guza & Inman (1975) show that the number of edge-wave antinodes sometimes alternated between adjacent integers. This phenomenon has yet to be explained.

In this paper, the above two problems are studied. As to the first one, the beach geometry is found to introduce an additional detuning term to the governing equations which affects the edge-wave dynamics. As to the second problem, the stability of all possible steady state standing edge-wave modes to large-scale disturbances is first examined. Regions of stable and unstable modes are analytically specified. The unstable mode found by Akylas (1983) is shown to fall in the unstable-mode region. The significance of these stable and unstable modes is also discussed.

Finally, numerical calculations of the equations governing the large-scale edge-wave modulations are carried out. The antinode-number alternation phenomenon is found in the numerical results. The nonlinear evolution of edge waves on a wide beach is commented on at the end of this paper.

2 Formulation

Equations governing the edge-wave amplitudes are a little different on a wide bounded beach and on an open beach. We treat them separately.

2.1 Edge waves on an open beach

Consider a normally incident and strongly-reflected wavetrain of frequency ω interacting with two Stokes edge-wave packets of frequency $\frac{1}{2}\omega$ propagating in opposite directions along an open beach of angle α. The undisturbed incident wave and its reflexion is described by a potential

$$\phi_{inc} = \frac{ga}{\omega} S_1(x,y) e^{-i\omega t} + c.c., \tag{2.1}$$

where g is the gravitational acceleration, a is the amplitude scale of the incident wave, and $S_1(x,y)$ is a real-valued function. This incident-wave field will be modified when edge waves are excited.

Following Akylas (1983), a suitable expansion of the velocity potential for the two Stokes edge-wave packets and the incident wavetrain is of the form (dimensions have been restored except as noted)

$$\begin{aligned} \phi \;=\; & \frac{ga}{\omega}\{\epsilon^{-\frac{1}{2}} e^{-kx\ \cos\alpha + ky\ \sin\alpha}[A(X,Y,Z,T)e^{i(kz-\frac{1}{2}\omega t)} + B(X,Y,Z,T)e^{i(-kz-\frac{1}{2}\omega t)} + c.c.] \\ & +[S(x,y;X,Y,Z,T)e^{-i\omega t} + c.c.] + \text{higher order terms,}\} \end{aligned} \tag{2.2}$$

where

$$k = \frac{\omega^2}{4g\ \sin\alpha}, \qquad \epsilon = \frac{4ka}{\sin\alpha} = \frac{a\omega^2}{g\ \sin^2\alpha}, \ \text{ which is assumed small,} \tag{2.3}$$

$$X = \mu 4kx, \ \ Y = \mu 4ky, \ \ Z = \mu 4kz, \ \ T = \mu\omega t, \tag{2.4}$$

and $\mu^{-1} \gg 1$ is the dimensionless modulation scale.

A multiple-scale perturbation method is used to determine the evolution of the edge-wave amplitudes A and B. It is found that A, B satisfy the following equations on the shoreline:

$$A_T + A_Z = -i\mu A_{ZZ} + \frac{\epsilon}{\mu}\{\frac{1}{2}\ \cos\alpha\chi(\alpha)S_0 B^* - \frac{i}{128}A^2A^* + \delta BB^*A\} \quad (X=0, Y=0) \tag{2.5}$$

$$B_T - B_Z = -i\mu B_{ZZ} + \frac{\epsilon}{\mu}\{\frac{1}{2}\ \cos\alpha\chi(\alpha)S_0 A^* - \frac{i}{128}B^2B^* + \delta AA^*B\} \quad (X=0, Y=0) \tag{2.6}$$

where

$$S_0 = S_1(0,0), \tag{2.7}$$

$$\chi(\alpha)S_0 = k\int_0^\infty S_1(x,0)e^{-2kx\ \cos\alpha}dx, \tag{2.8}$$

and when $\alpha = 2\pi/N$,

$$\delta = \frac{1}{64}\{-32N\chi^2\ \sin 2\alpha + i(3 + \frac{32N\ \sin 2\alpha}{\pi}\int_0^\infty \frac{C_l^2}{l-\omega^2}dl)\}, \tag{2.9}$$

where the integral in (2.9) is to be interpreted as a principle value. (See Minzoni & Whitham 1977)

If the beach-angle α is small, χ and δ can be evaluated asymptotically (see Minzoni & Whitham 1977, Akylas 1983):

$$\chi(\alpha) \sim \frac{1}{2e^2}, \quad \delta(\alpha) \sim \frac{1}{256}(-1.8413 + 0.4942i) = -0.72 \times 10^{-2} + 0.19 \times 10^{-2} i \quad (\alpha \to 0). \tag{2.10}$$

When the balance $\epsilon = \mu$ is chosen, the dispersive terms in equations (2.5) and (2.6) are relatively small and can be neglected. Further, if we simply denote $\frac{1}{2}\cos\alpha\chi(\alpha)S_0$ as S_0, equations for A and B on the shoreline $(X = 0, Y = 0)$ will reduce to

$$A_T + CgA_Z = S_0B^* + i\gamma A^2A^* + \delta BB^*A \tag{2.11}$$

$$B_T - CgB_Z = S_0A^* + i\gamma B^2B^* + \delta AA^*B \tag{2.12}$$

where

$$Cg = 1, \quad \gamma = -\frac{1}{128}i, \tag{2.13}$$

and δ is as given by (2.9), or (2.10) if the beach angle α is small.

2.2 Edge waves on a wide bounded beach

When the beach is wide but bounded by two sidewalls normal to the shoreline, the forced edge-wave wavelength and the free edge-wave wavelength mismatch will also affect the dynamics of edge waves.

Consider a beach of angle α, which is bounded by two sidewalls at $z = 0$ and $z = b$. A normally incident wave of frequency ω comes to the shore and is strongly reflected. The generated edge wave has the primary wavenumber $k_0 = \frac{N\pi}{b}$, where N is the number of the coastline edge-wave antinodes and is assumed to be large. This edge wave is both temporally and spatially modulated.

Suppose the undisturbed incident wave field is described by a potential

$$\phi_{inc} = \frac{ga}{\omega}S_1(x,y)e^{-i\omega t} + c.c., \tag{2.14}$$

where $S_1(x, y)$ is a real-valued function, and a is the incident-wave amplitude scale which is assumed small. Introduce the small perturbation parameter

$$\epsilon = \frac{a\omega^2}{g\,\sin^2\alpha}, \tag{2.15}$$

and assume that

$$\epsilon N = h \sim O(1), \tag{2.16}$$

where h is a dimensionless measure of the beach width. The suitable expansion of the velocity potential for the edge-wave packets and the incident wave is of the following dimensional form:

$$\begin{aligned}\phi &= \frac{ga}{\omega}\{\epsilon^{-\frac{1}{2}}e^{-kx\ \cos\alpha+ky\ \sin\alpha}[A(X,Y,Z,T)e^{i(k_0 z-\frac{1}{2}\omega t)}+B(X,Y,Z,T)e^{i(-k_0 z-\frac{1}{2}\omega t)}+c.c.]\\ &\quad +[S(x,y;X,Y,Z,T)e^{-i\omega t}+c.c.]+\text{higher order terms},\}\end{aligned} \tag{2.17}$$

where

$$k=\frac{\omega^2}{4g\ \sin\alpha},\qquad k_0=\frac{N\pi}{b}, \tag{2.18}$$

$$X=\epsilon\, 4kx,\ \ Y=\epsilon\, 4ky,\ \ Z=\epsilon\, 4k_0 z,\ \ T=\epsilon\,\omega t. \tag{2.19}$$

A similar perturbation analysis results in the following equations for A and B on the shoreline $(X=0, Y=0)$:

$$A_T+A_Z=iJA+S_0B^*+i\gamma A^2A^*+\delta BB^*A \tag{2.20}$$

$$B_T-B_Z=iJB+S_0A^*+i\gamma B^2B^*+\delta AA^*B \tag{2.21}$$

$$A=B,\qquad Z=0,4\pi h \tag{2.22}$$

where

$$J=\frac{1-\frac{k_0}{k}}{4\epsilon}\ \text{is the detuning parameter}, \tag{2.23}$$

$$\gamma=-\frac{i}{128},\quad \delta=\frac{1}{64}\{-32N\chi^2\ \sin 2\alpha+i(3+\frac{32N\ \sin 2\alpha}{\pi}\int_0^\infty\frac{C_l^2}{l-\omega^2}dl)\}. \tag{2.24}$$

With a stretching of the Z coordinate, the above equations can be rewritten as

$$A_T+CgA_Z=iJA+S_0B^*+i\gamma A^2A^*+\delta BB^*A \tag{2.25}$$

$$B_T-CgB_Z=iJB+S_0A^*+i\gamma B^2B^*+\delta AA^*B \tag{2.26}$$

$$A=B,\qquad Z=0,\pi \tag{2.27}$$

$$\text{with}\quad C_g=\tfrac{1}{4h}. \tag{2.28}$$

It needs to be pointed out that the value of C_g depends on the actual width of the beach. If the beach is very wide, C_g will be quite small.

When the beach-angle α is small,

$$\gamma=-\frac{i}{128},\quad \delta=-0.72\times10^{-2}+0.19\times10^{-2}i. \tag{2.29}$$

Dissipation may be introduced by adding a linear damping term to the equations (2.25) and (2.26).

3 Steady state standing edge waves and their stability

On a bounded beach, since the possible free edge-wave frequencies are far apart, an incident wave will only be able to excite a single subharmonic standing edge wave, if any. When it does, this edge wave will reach a steady final state (see Guza & Inman 1975, Minzoni & Whitham 1977). But if the beach is open or bounded but wide, since the possible resonant frequencies are so close together, an incident wave usually can excite several adjacent standing edge-wave modes, so that the large-scale amplitude modulations will arise. If this is the case, there are serious and important questions as to how edge waves evolve and what their final states may be.

A first step toward answering these questions is to study the stability of steady state standing edge-wave modes to large-scale disturbances. The equations governing these large-scale disturbances on the shoreline are as derived earlier. If dissipation is also included, they take the form

$$A_T + CgA_Z = i(J + iL)A + S_0B^* + i\gamma A^2A^* + \delta BB^*A \tag{3.1}$$

$$B_T - CgB_Z = i(J + iL)B + S_0A^* + i\gamma B^2B^* + \delta AA^*B \tag{3.2}$$

$$(A = B, \quad Z = 0, \pi \qquad \text{on a wide bounded beach})$$

where J is the detuning parameter, (on an open beach, $J = 0$,) and $L > 0$ is the linear damping coefficient. Physical arguments show that $\mathrm{Re}(\delta) < 0$.

3.1 Steady state standing edge waves

The steady state standing edge-waves are described by

$$\begin{aligned} A &= a_K e^{-iKZ}, \\ B &= a_K e^{iKZ}, \end{aligned} \tag{3.3}$$

where K is any integer if the beach is wide but bounded, any real number if it is unbounded (or open). Each K represents one steady state standing edge-wave mode. a_K is a constant and is determined by the equation

$$i(J + KC_g + iL)a_K + S_0a_K^* + (\delta + i\gamma)a_K^2a_K^* = 0. \tag{3.4}$$

If $a_K = re^{i\theta}$, it is a simple matter to show that r is given by

$$r^2 = \frac{L\delta_r - (J + KC_g)(\delta_i + \gamma) + \sqrt{S_0^2|\delta + i\gamma|^2 - [L(\delta_i + \gamma) + (J + KC_g)\delta_r]^2}}{|\delta + i\gamma|^2}, \tag{3.5}$$

and θ is given by the equation

$$-i(J + KC_g) + L - (\delta + i\gamma)r^2 = S_0e^{-2i\theta}, \tag{3.6}$$

where δ_r and δ_i are the real and imaginary parts of δ.

Clearly such steady edge waves exist only for a limited range of the parameter combination $J+KC_g$. If $\delta_i+\gamma<0$, which is the case for small-angle beaches, such steady states exist only when

$$-\sqrt{S_0^2-L^2}\equiv\bar{J}_{min}<J+KC_g<\bar{J}_{max}\equiv\frac{|S_0(\delta+i\gamma)|-|L(\delta_i+\gamma)|}{|\delta_r|}. \tag{3.7}$$

If $\delta_i+\gamma>0$, such steady states exist when

$$-\frac{|S_0(\delta+i\gamma)|-|L(\delta_i+\gamma)|}{|\delta_r|}\equiv\bar{J}_{min}<J+KC_g<\bar{J}_{max}\equiv\sqrt{S_0^2-L^2}. \tag{3.8}$$

3.2 Linear stability analysis

The stability of the steady mode (3.3) with $K=0$ on an open beach was studied by Akylas (1983) and was found to be unstable to large-scale disturbances. Now we study the stability of all possible steady modes of the form (3.3) on both wide bounded and open beaches.

Assume that A,B as given by (3.3) are slightly disturbed and are written as

$$\begin{aligned}A&=(a_K+\tilde{a}(Z,T))e^{-iKZ}\\B&=(a_K+\tilde{b}(Z,T))e^{iKZ}\end{aligned} \tag{3.9}$$

where $\tilde{a},\tilde{b}$ are infinitesimal disturbances. After (3.9) is substituted into the equations (3.1), (3.2) and higher order terms neglected, $\tilde{a},\tilde{b}$ are found to satisfy the following linear equations

$$\tilde{a}_T+Cg\tilde{a}_Z=[i(J+KCg+iL)+(\delta+2i\gamma)a_Ka_K^*]\tilde{a}+i\gamma a_K^2\tilde{a}^*+\delta a_Ka_K^*\tilde{b}+(S_0+\delta a_K^2)\tilde{b}^* \tag{3.10}$$

$$\tilde{b}_T-Cg\tilde{b}_Z=[i(J+KCg+iL)+(\delta+2i\gamma)a_Ka_K^*]\tilde{b}+i\gamma a_K^2\tilde{b}^*+\delta a_Ka_K^*\tilde{a}+(S_0+\delta a_K^2)\tilde{a}^* \tag{3.11}$$

$$(\tilde{a}=\tilde{b},\quad Z=0,\pi\qquad\text{on a wide bounded beach})$$

With the notation $\tilde{c}\equiv\tilde{a}^*,\tilde{d}\equiv\tilde{b}^*$, equations for $\tilde{a},\tilde{b},\tilde{c}$ and $\tilde{d}$ are easily obtained from (3.10) and (3.11) to be

$$\begin{aligned}\tilde{a}_T+Cg\tilde{a}_Z=&\ [i(J+KCg+iL)+(\delta+2i\gamma)a_Ka_K^*]\tilde{a}+\delta a_Ka_K^*\tilde{b}+i\gamma a_K^2\tilde{c}+(S_0+\delta a_K^2)\tilde{d}\\ \tilde{b}_T-Cg\tilde{b}_Z=&\ [i(J+KCg+iL)+(\delta+2i\gamma)a_Ka_K^*]\tilde{b}+\delta a_Ka_K^*\tilde{a}+i\gamma a_K^2\tilde{d}+(S_0+\delta a_K^2)\tilde{c}\\ \tilde{c}_T+Cg\tilde{c}_Z=&\ -i\gamma a_K^{*2}\tilde{a}+(S_0+\delta a_K^2)^*\tilde{b}+[i(J+KCg+iL)+(\delta+2i\gamma)a_Ka_K^*]^*\tilde{c}+\delta^*a_Ka_K^*\tilde{d}\\ \tilde{d}_T-Cg\tilde{d}_Z=&\ -i\gamma a_K^{*2}\tilde{b}+(S_0+\delta a_K^2)^*\tilde{a}+[i(J+KCg+iL)+(\delta+2i\gamma)a_Ka_K^*]^*\tilde{d}+\delta^*a_Ka_K^*\tilde{c}\\ &(\tilde{a}=\tilde{b},\quad Z=0,\pi\qquad\text{on a wide bounded beach})\\ &(\tilde{c}=\tilde{d},\quad Z=0,\pi\qquad\text{on a wide bounded beach})\end{aligned} \tag{3.12}$$

With the following change of variables

$$\begin{aligned}W_1&=\tilde{a}+\tilde{b},\\W_2&=\tilde{a}-\tilde{b},\\W_3&=\tilde{c}+\tilde{d},\\W_4&=\tilde{c}-\tilde{d},\end{aligned} \tag{3.13}$$

W_1, W_2, W_3, W_4 are found to satisfy the equations

$$\begin{aligned} W_{1T} + C_g W_{2Z} = &\ [i(J + KC_g + iL) + (2\delta + 2i\gamma)a_K a_K^*]W_1 + (S_0 + (\delta + i\gamma)a_K^2)W_3 \\ W_{2T} + C_g W_{1Z} = &\ [i(J + KC_g + iL) + 2i\gamma a_K a_K^*]W_2 + ((i\gamma - \delta)a_K^2 - S_0)W_4 \\ W_{3T} + C_g W_{4Z} = &\ (S_0 + (\delta + i\gamma)a_K^2)^* W_1 + [i(J + KC_g + iL) + (2\delta + 2i\gamma)a_K a_K^*]^* W_3 \\ W_{4T} + C_g W_{3Z} = &\ ((i\gamma - \delta)a_K^2 - S_0)^* W_2 + [i(J + KC_g + iL) + 2i\gamma a_K a_K^*]^* W_4 \\ &\ (W_2 = 0, \ \ Z = 0, \pi \quad \text{on a wide bounded beach}) \\ &\ (W_4 = 0, \ \ Z = 0, \pi \quad \text{on a wide bounded beach}) \end{aligned} \tag{3.14}$$

Due to the boundary conditions, the normal mode analysis takes slightly different forms on an open beach and on a wide bounded beach.

1. On an open beach, the conventional normal mode analysis assumes that

$$\begin{aligned} W_1 &= \overline{W}_1 e^{imZ+\sigma T} \\ W_2 &= \overline{W}_2 e^{imZ+\sigma T} \\ W_3 &= \overline{W}_3 e^{imZ+\sigma T} \\ W_4 &= \overline{W}_4 e^{imZ+\sigma T} \end{aligned} \tag{3.15}$$

   where the disturbance wavenumber m takes on any real value.

   The eigenvalue σ is related to the wavenumber m by the equation

$$\begin{vmatrix} P_1 - \sigma & P_2 & -imC_g & 0 \\ P_2^* & P_1^* - \sigma & 0 & -imC_g \\ -imC_g & 0 & P_3 - \sigma & P_4 \\ 0 & -imC_g & P_4^* & P_3^* - \sigma \end{vmatrix} = 0, \tag{3.16}$$

   Where

$$\begin{aligned} P_1 &= P_1(K) = i(J + KCg) - L + 2(\delta + i\gamma)a_K a_K^* \\ P_2 &= P_2(K) = S_0 + (\delta + i\gamma)a_K^2 \\ P_3 &= P_3(K) = i(J + KCg) - L + 2i\gamma a_K a_K^* \\ P_4 &= P_4(K) = (i\gamma - \delta)a_K^2 - S_0 \end{aligned} \tag{3.17}$$

   and a_K is as given by the equation (3.4).

   Notice that

$$P_2 = -\frac{(iJ - L)a_K}{a_K^*}, \qquad P_4 = \frac{a_K}{a_K^*} P_3 \tag{3.18}$$

   due to the equation (3.4).

2. On a wide bounded beach, due to the sidewall boundary conditions, the normal mode analysis assumes that

$$\begin{aligned} W_1 &= \overline{W}_1 \ \cos\ mZ\, e^{\sigma T} \\ W_2 &= \overline{W}_2 \ \sin\ mZ\, e^{\sigma T} \\ W_3 &= \overline{W}_3 \ \cos\ mZ\, e^{\sigma T} \\ W_4 &= \overline{W}_4 \ \sin\ mZ\, e^{\sigma T} \end{aligned} \tag{3.19}$$

   where the disturbance wavenumber m takes on any integer value.

   The eigenvalue σ is related to the wavenumber m by the equation

$$\begin{vmatrix} P_1 - \sigma & P_2 & -mC_g & 0 \\ P_2^* & P_1^* - \sigma & 0 & -mC_g \\ mC_g & 0 & P_3 - \sigma & P_4 \\ 0 & mC_g & P_4^* & P_3^* - \sigma \end{vmatrix} = 0, \tag{3.20}$$

and P_1, P_2, P_3, P_4 are as given by (3.17).

After some algebra, it is found that (3.16) and (3.20) lead to the same quartic equation for σ:

$$\begin{aligned}&\sigma^4 - [P_1 + P_1^* - 2L]\sigma^3 + [P_1P_1^* - P_2P_2^* - 2L(P_1 + P_1^*) + 2(mCg)^2]\sigma^2 \\ &-[(mCg)^2(P_1 + P_1^* - 2L) - 2L(P_1P_1^* - P_2P_2^*)]\sigma \\ &+(mCg)^2[P_1P_3 + (P_1P_3)^* + P_2P_4^* + P_2^*P_4 + (mCg)^2] = 0.\end{aligned} \tag{3.21}$$

From (3.4) and (3.17), it is readily shown that

$$\begin{aligned}&P_1 + P_1^* = -2L + 4\delta_r a_K a_K^* \quad (< 0), \\ &P_1P_1^* - P_2P_2^* = 4a_K a_K^* \sqrt{S_0^2|\delta + i\gamma|^2 - [L(\delta_i + \gamma) + (J + KC_g)\delta_r]^2} \quad (> 0), \\ &P_1P_3 + (P_1P_3)^* + P_2P_4^* + P_2^*P_4 = -4[L\delta_r a_K a_K^* + (J + KC_g + (\delta_i + \gamma)a_K a_K^*)(J + KC_g + 2\gamma a_K a_K^*)].\end{aligned} \tag{3.22}$$

4 Stability results

A steady edge-wave mode (3.3) is possible if $\bar{J}_{min} < J + KC_g < \bar{J}_{max}$, with $\bar{J}_{min}$ and $\bar{J}_{max}$ given by (3.7) or (3.8). It is unstable if some normal-mode disturbances are unstable, and vise versa. A normal-mode disturbance is unstable if its eigenvalue σ has a positive real part; it is stable otherwise. In the present situation, σ is a root of the quartic equation (3.21). To solve (3.21) for general values of K and m looks complicated, but actually it is not difficult. For our purpose, it is not necessary to solve (3.21). The signs of $\mathrm{Re}(\sigma)$ can be determined by simply examining the coefficients of the equation (3.21). The results are given below. (The derivation is given in Appendix 1.)

I. If the edge-wave mode (3.3) is such that $P_1P_3 + (P_1P_3)^* + P_2P_4^* + P_2^*P_4 < 0$, it is unstable. The unstable disturbance wavenumbers m are confined to the interval

$$0 < m^2C_g^2 < m_1^2C_g^2 \equiv -(P_1P_3 + (P_1P_3)^* + P_2P_4^* + P_2^*P_4). \quad (4.1)$$

These unstable disturbances are standing waves of growing amplitudes because they have positive real eigenvalues σ.

II. If the edge-wave mode (3.3) is such that $0 < P_1P_3 + (P_1P_3)^* + P_2P_4^* + P_2^*P_4 < P_1P_1^* - P_2P_2^* - 2L(P_1 + P_2)$, it is stable.

III. If the edge-wave mode (3.3) is such that $P_1P_3 + (P_1P_3)^* + P_2P_4^* + P_2^*P_4 > P_1P_1^* - P_2P_2^* - 2L(P_1 + P_2)$, it is unstable. The unstable disturbances have wavenumbers m such that

$$m^2C_g^2 > m_2^2C_g^2 \quad (4.2)$$

where

$$m_2^2C_g^2 \equiv -\frac{2L(P_1P_1^* - P_2P_2^*)(P_1 + P_2)(\frac{P_1P_1^* - P_2P_2^*}{P_1+P_2-2L} - 2L)}{(P_1 + P_2 - 2L)\{(P_1P_3 + (P_1P_3)^* + P_2P_4^* + P_2^*P_4) - (P_1P_1^* - P_2P_2^* - 2L(P_1 + P_2))\}}. \quad (4.3)$$

These unstable disturbances are travelling waves of growing amplitudes since their eigenvalues σ are complex.

We can further show from the equation (3.21) that the eigenvalue

$$\sigma \longrightarrow \pm mC_gi + \sigma^{(0)} \qquad \text{as } mC_g \longrightarrow \infty, \quad (4.4)$$

where $\sigma^{(0)}$ is the root of the quadratic equation

$$\sigma^{(0)2} - \frac{P_1 + P_1^* - 2L}{2}\sigma^{(0)} - \frac{[P_1P_3 + (P_1P_3)^* + P_2P_4^* + P_2^*P_4] - [P_1P_1^* - P_2P_2^* - 2L(P_1 + P_2)]}{4} = 0. \quad (4.5)$$

The derivation of (4.4) and (4.5) is given in Appendix 2.

In this third case, because $P_1P_3 + (P_1P_3)^* + P_2P_4^* + P_2^*P_4 > P_1P_1^* - P_2P_2^* - 2L(P_1 + P_2)$, one root of the equation (4.5) is real and positive and the other one is real and negative. The unstable disturbance takes the positive $\sigma^{(0)}$. Since $\sigma^{(0)}$ is independent of mC_g, very short disturbance waves tend to have the same growth rate $\sigma^{(0)}$.

It should be noticed that edge-wave modes of this kind are very unusual, because they are unstable to small-scale disturbances. Interpretation of existence of these modes requires caution and will be discussed later.

The above stability results are not affected to any degree by a proportional change of γ and δ, and it is easy to show that

$$\sigma(\beta\gamma, \beta\delta) = \sigma(\gamma, \delta). \tag{4.6}$$

A change in S_0 causes σ to change in a simple way:

$$\sigma(\beta m, \beta S_0, \beta L, \beta(J + KC_g)) = \beta\sigma(m, S_0, L, (J + KC_g)). \tag{4.7}$$

These facts are helpful to determine the stability structure when different values of γ, δ and S_0 are taken.

The above general stability results immediately give the precise stability structure of steady state standing edge-wave modes on a given beach. As an example, we determine this structure on a mildly sloping beach.

On a mildly sloping beach,

$$\gamma = -\frac{1}{128}, \quad \delta = -0.72 \times 10^{-2} + 0.19 \times 10^{-2} i. \tag{4.8}$$

The damping coefficient L is small but hard to determine. It is usually set to be zero for simplicity.

In this case, since $\delta_i + \gamma < 0$, $\bar{J}_{min}$ and $\bar{J}_{max}$ are given by the equation (3.7) as

$$\bar{J}_{min} = -\sqrt{S_0^2} = -S_0, \qquad \bar{J}_{max} = \frac{|S_0(\delta + i\gamma)|}{|\delta_r|} = 1.29 S_0. \tag{4.9}$$

Steady edge-wave modes (3.3) are possible if

$$-S_0 < J + KC_g < 1.29 S_0. \tag{4.10}$$

The stability structure is as shown in Figure 1.

Region I : $-S_0 < J + KC_g < 0.82 S_0$.

The steady edge-wave modes in this region are unstable. From the equations (3.22) and (4.1) we get

$$m_1^2 C_g^2 = 4(J + KC_g + (\delta_i + \gamma) a_K a_K^*)(J + KC_g + 2\gamma a_K a_K^*), \tag{4.11}$$

where

$$a_K a_K^* = \frac{-(J + KC_g)(\delta_i + \gamma) + \sqrt{S_0^2 |\delta + i\gamma|^2 - (J + KC_g)^2 \delta_r^2}}{|\delta + i\gamma|^2}. \tag{4.12}$$

Values of $m_1 C_g$ are plotted against $J + KC_g$ in Figure 1. The unstable disturbance wavenumbers m are confined in the interval:

$$0 < m^2 C_g^2 < m_1^2 C_g^2. \tag{4.13}$$

These disturbances are standing waves of growing amplitudes.

Region II : $0.82 S_0 < J + KC_g < 1.24 S_0$.

The steady edge-wave modes in this region are stable.

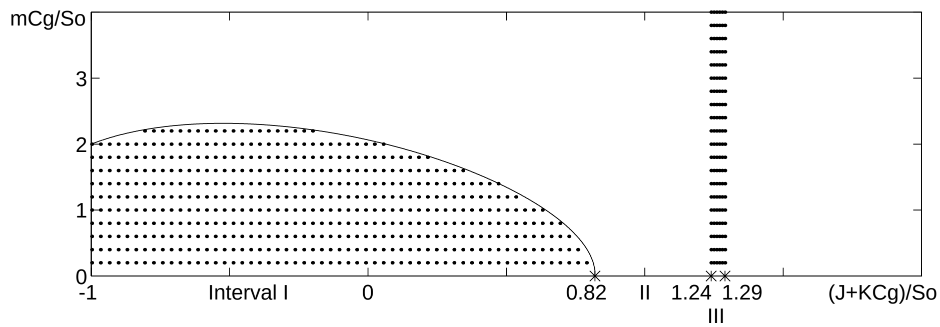

Figure 1: regions of stable and unstable steady edge-wave modes (3.3) and regions of their stable and unstable disturbances on a mildly sloping beach. The unstable steady modes (3.3) are in the region I and III. The unstable disturbances are in the dotted area.

Region III : $1.24S_0 < J + KC_g < 1.29S_0$.

The steady edge-wave modes in this region are unstable. $m_2^2C_g^2$ is given by the equations (3.22) and (4.3). Since $L = 0$, $m_2C_g = 0$. Any disturbances with $m^2C_g^2 > 0$ are unstable, and they are travelling waves of growing amplitudes.

The unstable edge-wave mode Akylas (1983) found on an open, mildly sloping beach corresponds to the one in Region I with $J = 0, K = 0$ and $L = 0$. With $S_0 = \frac{1}{4e^2}$ taken, he numerically determined that

$$m_1Cg \approx 0.052,$$

and found that the eigenvalues σ of the unstable disturbances have very small imaginary parts.

Actually, for this mode, (4.11) and (4.12) give

$$a_0a_0^* = \frac{S_0}{|\delta + i\gamma|}, \tag{4.14}$$

$$\begin{aligned} m_1^2C_g^2 &= 8\gamma(\delta_i + \gamma)(a_Ka_K^*)^2 \\ &= \frac{8\gamma(\delta_i + \gamma)S_0^2}{|\delta + i\gamma|^2} \\ &= 0.49 \times 10^{-2}. \end{aligned} \tag{4.15}$$

Therefore, the exact value for m_1C_g is

$$m_1Cg = 0.070. \tag{4.16}$$

This value can be checked in Figure 1. Moreover, the eigenvalues σ of the unstable disturbances are exactly real and positive, thus they represent standing waves of growing amplitudes.

Different values of γ, δ, L will slightly change the parameters in Figure 1 and m_1C_g and m_2C_g, but the basic stability structure (as in Figure 1) does not change.

The above stability structure has two distinctive features:

1. Although many steady state standing edge-wave modes of the form (3.3) are unstable to large-scale modulations (region I in Figure 1), some of them are stable (region II in Figure 1). These stable ones are an attracting set and will strongly affect the dynamics of edge-wave evolutions.

2. There exists a small region of steady state standing edge-wave modes which are unstable to very short modulational disturbances (region III in Figure 1). This may seem to suggest a mechanism of short-wave excitation by a long wave. If it really occurs in edge waves, it will invalidate the edge-wave modulational equations we derived before. But more likely is that these short disturbances are excited because dispersion is neglected. When the small dispersive terms are included, these short disturbances will likely be suppressed.

5 Nonlinear evolution of edge waves on a wide beach

The above results on the stability of steady state standing edge waves provide some insight on the nonlinear evolution of edge waves. On a wide bounded beach, the steady edge-wave modes of the form (3.3) are discrete. The number of stable and unstable such modes depends on C_g and J in the equations (2.25) and (2.26). Since stable steady modes form an attracting set, if they exist and are excited, the edge wave is likely to be attracted to one of these modes and settle down there. If they do not exist, the edge wave can not settle down to any steady mode, and its evolution will be quite different. In this case, one possibility is that the energy will mostly exchange among a few adjacent discrete modes, and the edge wave will evolve into a limit cycle. This corresponds to the antinode-number alternation phenomenon observed in Guza & Inman (1975)'s experiments.

To further investigate the edge-wave evolution on a wide bounded beach, numerical calculations are carried out for the governing equations (2.25), (2.26) and (2.27). To facilitate the computation, A, B are decomposed in the following form:

$$A = \sum_{K=-\infty}^{\infty} a_K(T)\, e^{-iKZ}, \tag{5.1}$$

$$B = \sum_{K=-\infty}^{\infty} a_K(T)\, e^{iKZ}. \tag{5.2}$$

When this decomposition is substituted into the equations (2.25), (2.26) and (2.27), an infinite-dimensional dynamical system for $a_K(T)$ are obtained. Truncation of this system is necessary for any numerical calculations. The choice for the number of a_K's depends on the accuracy required.

For easy comparison with the previous stability results, we consider a beach of small angle α, where

$$\gamma = -\frac{1}{128}, \quad \delta = -0.72 \times 10^{-2} + 0.19 \times 10^{-2} i. \tag{5.3}$$

We also take

$$L = 0, \quad S_0 = \frac{1}{4e^2}. \tag{5.4}$$

Depending on the actual width of the beach, C_g and J may take different values.

For convenience, we normalize $S_0 = 1$, and other parameters change to

$$\gamma = -\frac{1}{128} \times 4e^2 = -0.23, \quad \delta = (-0.72 \times 10^{-2} + 0.19 \times 10^{-2} i) \times 4e^2 = -0.21 + 0.056i. \tag{5.5}$$

L is still zero. J and C_g are multiplied by $4e^2$ and are still denoted as J and C_g. A stretch of the T coordinate is also needed.

Initially, the edge waves are very small. They are excited by the incident wave. In our computation, we take small "white noise" initial conditions with

$$a_K(0) = 0.01 + 0.01i, \quad K = 0, \pm 1, \pm 2, \ldots \tag{5.6}$$

We also choose the following two sets of values of J and C_g. These two solution behaviors appear to be typical.

1. $J = 0, C_g = 1$:

   In this case, (4.10) shows that steady modes (3.3) exist for $K = 0$ and 1. The steady mode with $K = 0$ is unstable and the one with $K = 1$ is stable. At the initial stage of edge-wave generation, since the $K = 0$ mode is at exact subharmonic resonance, it quickly grows and reaches its steady state amplitude. But its steady state is unstable. It then gradually loses its energy to its side-band modes with $K = \pm 1$ and excites them. Notice that the steady mode with $K = 1$ is stable. When it is excited, it absorbs energy and attracts the edge wave to reach its own steady state. The edge wave finally settles down to this steady mode. The time-evolution of a_K's is plotted in Figure 2.

2. $J = 0.5, C_g = 1$:

   In this case, (4.10) shows that steady modes (3.3) exist for $K = -1$ and 0. These two steady modes are both unstable. Therefore, the edge wave can not settle down to any steady mode. Instead, it goes to a periodic state with energy largely confined to a few adjacent modes and exchanging among them, as is illustrated in Figure 3. Notice that this behavior corresponds to the antinode-number alternation phenomenon which was observed in Guza & Inman (1975)'s experiments.

The above two types of edge-wave evolution are very distinctive. They are both possible on a wide bounded beach. The actual beach geometry and the incident wave dictate which one should occur.

On a wider beach, C_g is smaller, and thus more stable and unstable steady modes (3.3) exist. Expectedly, in this situation, the dynamical system of a_K's will show richer behaviors. For instance, the edge wave not only may go to a steady (stable mode) state or a limit cycle, but also may evolve into a quasi-periodic or even chaotic state. These aspects still remain to be studied.

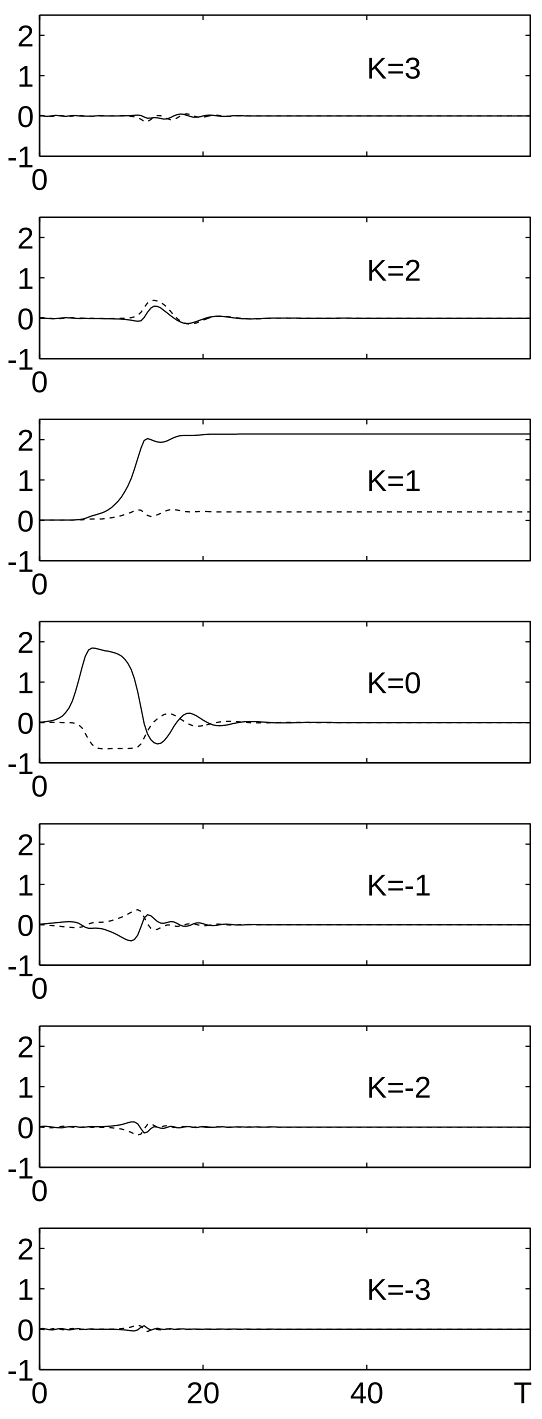

Figure 2: the time-evolution of a_K, $K = 0, \pm 1, \pm 2, \pm 3$. Parameters $J = 0, C_g = 1$. The solid line: $\mathrm{Re}(a_K)$; the dotted line: $\mathrm{Im}(a_K)$. This edge wave settles down to the stable steady mode (3.3) with $K = 1$.

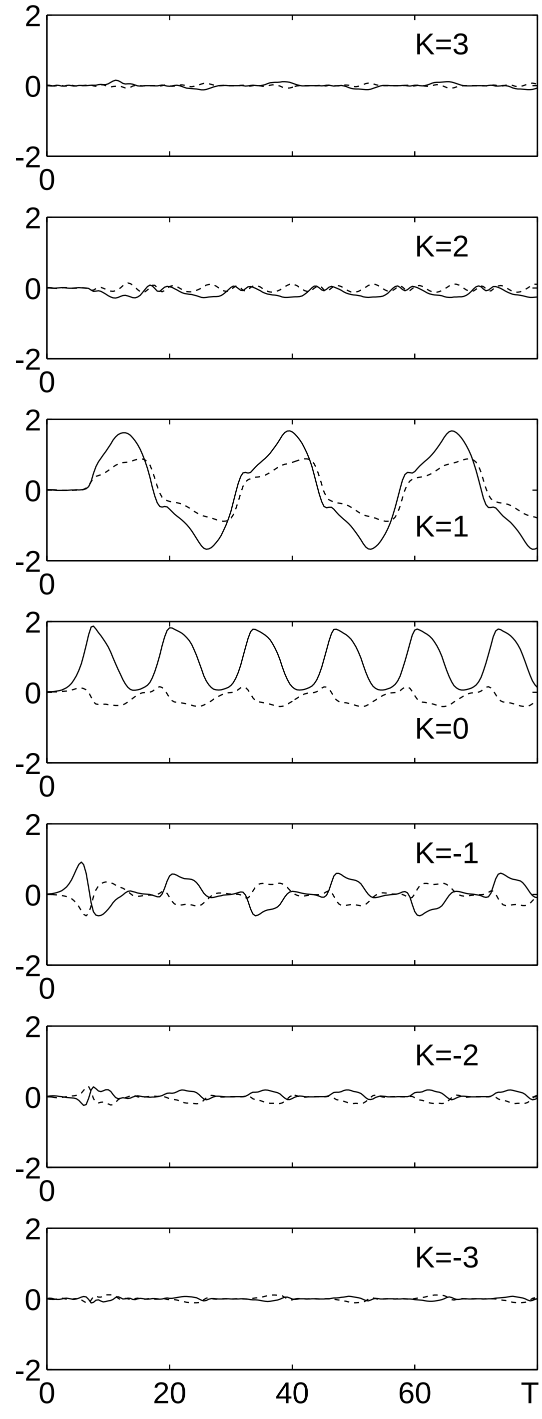

Figure 3: the time-evolution of a_K, $K = 0, \pm 1, \pm 2, \pm 3$. Parameters $J = 0.5, C_g = 1$. The solid line: $\mathrm{Re}(a_K)$; the dotted line: $\mathrm{Im}(a_K)$. This edge wave evolves into a limit cycle.

6 Summary

The stability of steady state standing edge waves to large-scale disturbances has been studied. Regions of stable and unstable edge-wave modes have been determined precisely, and the stability structure obtained analytically. The nonlinear evolution of edge waves on a wide beach has also been considered. An explanation has been found for the edge-wave antinode-number alternation phenomenon observed in Guza & Inman (1975)'s experiments.

Appendix 1. Root analysis of the quartic equation (3.21)

The quartic equation (3.21) is

$$\begin{aligned}&\sigma^4-[P_1+P_1^*-2L]\sigma^3+[P_1P_1^*-P_2P_2^*-2L(P_1+P_1^*)+2(mCg)^2]\sigma^2\\&-[(mCg)^2(P_1+P_1^*-2L)-2L(P_1P_1^*-P_2P_2^*)]\sigma\\&+(mCg)^2[P_1P_3+(P_1P_3)^*+P_2P_4^*+P_2^*P_4+(mCg)^2]=0,\end{aligned}\quad\text{(A1.1)}$$

Suppose the four roots are $\sigma_i, i=1,2,3,4$. Since the equation (A1.1) has real coefficients, complex roots only appear in conjugate pairs. It is well known that these four roots satisfy the following relations :

$$\sigma_1+\sigma_2+\sigma_3+\sigma_4 = P_1+P_1^*-2L \quad\text{(A1.2)}$$
$$(\sigma_1+\sigma_2)(\sigma_3+\sigma_4)+\sigma_1\sigma_2+\sigma_3\sigma_4 = P_1P_1^*-P_2P_2^*-2L(P_1+P_1^*)+2m^2C_g^2 \quad\text{(A1.3)}$$
$$\sigma_1\sigma_2(\sigma_3+\sigma_4)+\sigma_3\sigma_4(\sigma_1+\sigma_2) = m^2C_g^2(P_1+P_1^*-2L)-2L(P_1P_1^*-P_2P_2^*) \quad\text{(A1.4)}$$
$$\sigma_1\sigma_2\sigma_3\sigma_4 = m^2C_g^2(P_1P_3+(P_1P_3)^*+P_2P_4^*+P_2^*P_4+m^2C_g^2) \quad\text{(A1.5)}$$

Our purpose is to decide how the signs of the real parts of the roots depend on the coefficients in equation (A1.1).

Before doing the algebra, it should be noted from the equations (3.22) that

$$\begin{aligned}P_1+P_1^* &< 0,\\ P_1+P_1^*-2L &< 0,\\ P_1P_1^*-P_2P_2^* &> 0,\\ P_1P_1^*-P_2P_2^*-2L(P_1+P_2) &> 0.\end{aligned}\quad\text{(A1.6)}$$

These facts will be used in the following analysis.

1. If $P_1P_3+(P_1P_3)^*+P_2P_4^*+P_2^*P_4<0$:

   In this case, the root relation (A1.5) immediately tells us that at least one root is real positive when $m^2C_g^2<-(P_1P_3+(P_1P_3)^*+P_2P_4^*+P_2^*P_4)$. A further analysis will obtain more detailed information about these four roots.

   When $m^2C_g^2=0$, it is easy to show that

   $$\sigma_1=0, \qquad \sigma_2=-2L, \quad\text{(A1.7)}$$

   and σ_3, σ_4 are given by the quadratic equation

   $$\sigma^2-(P_1+P_1^*)\sigma+P_1P_1^*-P_2P_2^*=0. \quad\text{(A1.8)}$$

   Since

   $$P_1P_1^*-P_2P_2^*>0,$$

   and

   $$P_1+P_1^*<0,$$

   it is clear that $\mathrm{Re}(\sigma_3)<0, \quad \mathrm{Re}(\sigma_4)<0.$

When $m^2C_g^2$ gets larger but less than $-(P_1P_3 + (P_1P_3)^* + P_2P_4^* + P_2^*P_4)$, σ_1 will first move away from the origin along the positive $\mathrm{Re}(\sigma)$ axis, then it will change direction and move back to the origin along the positive $\mathrm{Re}(\sigma)$ axis. σ_2 always remains real and negative. σ_3 and σ_4 are always in the left half of the complex σ plane.

When $m^2C_g^2 = -(P_1P_3 + (P_1P_3)^* + P_2P_4^* + P_2^*P_4)$, $\sigma_1 = 0$ again.

When $m^2C_g^2 > -(P_1P_3 + (P_1P_3)^* + P_2P_4^* + P_2^*P_4)$, σ_1 moves onto the negative $\mathrm{Re}(\sigma)$ axis, and all four roots will stay in the left half of the complex σ plane.

To fully justify the above analysis, we need to prove that, as $m^2C_g^2$ changes, no roots will ever cross the $\mathrm{Im}(\sigma)$ axis onto the right half of the complex σ plane from the left half. This is proved by a contradiction argument. Suppose they do, then they either cross the $\mathrm{Im}(\sigma)$ axis at the origin or not at the origin.

- If they cross at the origin, the equation (A1.4) tells us that at most one root does that and this root remains on the real axis when it crosses from the left half plane to the right half. This will mean that $\sigma_1\sigma_2\sigma_3\sigma_4$ will change sign from positive to negative, which does not happen for any $m^2C_g^2$.
- If they do not cross at the origin, since complex roots appear in conjugate pairs, two roots of conjugate pair, say σ_3 and σ_4, will cross the line simultaneously and $\sigma_3 = -\sigma_4$. The root relations now become:

$$\begin{aligned}
\sigma_1 + \sigma_2 &= P_1 + P_1^* - 2L && \text{(A1.9)}\\
\sigma_1\sigma_2 + \sigma_3\sigma_4 &= P_1P_1^* - P_2P_2^* - 2L(P_1 + P_1^*) + 2m^2C_g^2 && \text{(A1.10)}\\
\sigma_3\sigma_4(\sigma_1 + \sigma_2) &= m^2C_g^2(P_1 + P_1^* - 2L) - 2L(P_1P_1^* - P_2P_2^*) && \text{(A1.11)}\\
\sigma_1\sigma_2\sigma_3\sigma_4 &= m^2C_g^2(P_1P_3 + (P_1P_3)^* + P_2P_4^* + P_2^*P_4 + m^2C_g^2) && \text{(A1.12)}
\end{aligned}$$

From equation (A1.9) and (A1.11) we obtain

$$\sigma_3\sigma_4 = m^2C_g^2 - \frac{2L(P_1P_1^* - P_2P_2^*)}{P_1 + P_1^* - 2L} \qquad \text{(A1.13)}$$

Therefore, from (A1.10) and (A1.12) we get

$$\sigma_1\sigma_2 = m^2C_g^2 + P_1P_1^* - P_2P_2^* - 2L(P_1 + P_1^*) + \frac{2L(P_1P_1^* - P_2P_2^*)}{P_1 + P_1^* - 2L} \qquad \text{(A1.14)}$$

$$\sigma_1\sigma_2 = m^2C_g^2 + \frac{m_2C_g^2(P_1P_3 + (P_1P_3)^* + P_2P_4^* + P_2^*P_4 + \frac{2L(P_1P_1^* - P_2P_2^*)}{P_1+P_1^*-2L})}{m^2C_g^2 - \frac{2L(P_1P_1^* - P_2P_2^*)}{P_1+P_1^*-2L}} \qquad \text{(A1.15)}$$

The above two equations are consistent only if there exists $m^2C_g^2$ such that

$$m^2C_g^2 = -\frac{2L(P_1P_1^* - P_2P_2^*)(P_1 + P_2)(\frac{P_1P_1^* - P_2P_2^*}{P_1+P_2-2L} - 2L)}{(P_1 + P_2 - 2L)\{(P_1P_3 + (P_1P_3)^* + P_2P_4^* + P_2^*P_4) - (P_1P_1^* - P_2P_2^* - 2L(P_1 + P_2))\}} \qquad \text{(A1.16)}$$

But such a value for $m^2C_g^2$ does not exist since the right hand side is negative.

The above analysis concludes that if $P_1P_3 + (P_1P_3)^* + P_2P_4^* + P_2^*P_4 < 0$,

- when $m^2C_g^2 < m_1^2C_g^2 \equiv -(P_1P_3 + (P_1P_3)^* + P_2P_4^* + P_2^*P_4)$, one root is real positive. The other three roots have negative real parts.

- When $m^2C_g^2 > m_1^2C_g^2$, all four roots have negative real parts.

2. If $P_1P_3 + (P_1P_3)^* + P_2P_4^* + P_2^*P_4 > 0$:
   In this case, when $m^2C_g^2 = 0$,
   $$\sigma_1 = 0, \quad \sigma_2 = -2L,$$
   and σ_3, σ_4 are given by
   $$\sigma^2 - (P_1 + P_1^*)\sigma + P_1P_1^* - P_2P_2^* = 0$$
   and $\mathrm{Re}(\sigma_3) < 0, \mathrm{Re}(\sigma_4) < 0$ as discussed before.
   When $m^2C_g^2 > 0$ and small, since $\sigma_1\sigma_2\sigma_3\sigma_4 > 0$, σ_1 will move onto the negative $\mathrm{Re}(\sigma)$ axis, while σ_2 remains real negative. σ_3 and σ_4 are somewhere in the left half of the complex σ plane. So the four roots all have negative real parts. As $m^2C_g^2$ gets larger, the main interest is whether some roots could cross the $\mathrm{Im}(\sigma)$ axis into the right half plane. If they do, since $\sigma_1\sigma_2\sigma_3\sigma_4$ is now always positive, they could not cross through the origin and have to cross over from somewhere else on the $\mathrm{Im}(\sigma)$ axis. The analysis for the case $P_1P_3+(P_1P_3)^*+P_2P_4^*+P_2^*P_4 < 0$ shows that when the roots cross the imaginary axis, $m^2C_g^2$ has to be
   $$m^2C_g^2 = -\frac{2L(P_1P_1^* - P_2P_2^*)(P_1+P_2)(\frac{P_1P_1^*-P_2P_2^*}{P_1+P_2-2L} - 2L)}{(P_1+P_2-2L)\{(P_1P_3+(P_1P_3)^*+P_2P_4^*+P_2^*P_4) - (P_1P_1^* - P_2P_2^* - 2L(P_1+P_2))\}} \tag{A1.17}$$

   - When $P_1P_3+(P_1P_3)^*+P_2P_4^*+P_2^*P_4 > P_1P_1^* - P_2P_2^* - 2L(P_1+P_2)$, the right hand side of (A1.17) is positive, and such a value for $m^2C_g^2$ exists. When $m^2C_g^2$ gets larger than this value, the conjugate pair of roots will cross the imaginary axis onto the right half plane from somewhere other than the origin. As $m^2C_g^2$ gets even larger, this root pair will stay in the right half plane and will not move back onto the left half plane. The equations (A1.2) and (A1.5) show that the other two roots stays in the left half plane for all values of $m^2C_g^2$.
   - When $P_1P_3+(P_1P_3)^*+P_2P_4^*+P_2^*P_4 < P_1P_1^* - P_2P_2^* - 2L(P_1+P_2)$, the right hand side of (A1.17) is negative, and such a value for $m^2C_g^2$ does not exist. Thus the roots can not cross the imaginary axis and they always stay in the left half plane.

The above analysis concludes that

- If $P_1P_3+(P_1P_3)^*+P_2P_4^*+P_2^*P_4 > P_1P_1^* - P_2P_2^* - 2L(P_1+P_2)$, denoting
  $$m_2^2C_g^2 \equiv -\frac{2L(P_1P_1^* - P_2P_2^*)(P_1+P_2)(\frac{P_1P_1^*-P_2P_2^*}{P_1+P_2-2L} - 2L)}{(P_1+P_2-2L)\{(P_1P_3+(P_1P_3)^*+P_2P_4^*+P_2^*P_4) - (P_1P_1^* - P_2P_2^* - 2L(P_1+P_2))\}} \tag{A1.18}$$
  then, when
  $$m^2C_g^2 < m_2^2C_g^2, \tag{A1.19}$$
  all four roots have negative real parts. When
  $$m^2C_g^2 > m_2^2C_g^2, \tag{A1.20}$$
  two complex roots of conjugate pair have positive real parts, and the other two roots have negative real parts.
- If $0 < P_1P_3+(P_1P_3)^*+P_2P_4^*+P_2^*P_4 < P_1P_1^* - P_2P_2^* - 2L(P_1+P_2)$, all four roots have negative real parts.

Appendix 2. The asymptotic behavior of the roots σ of the quartic equation (3.21) for large values of mC_g

The quartic equation (3.21) is:

$$\begin{aligned}&\sigma^4 - [P_1 + P_1^* - 2L]\sigma^3 + [P_1 P_1^* - P_2 P_2^* - 2L(P_1 + P_1^*) + 2(mCg)^2]\sigma^2 \\ &-[(mCg)^2(P_1 + P_1^* - 2L) - 2L(P_1 P_1^* - P_2 P_2^*)]\sigma \\ &+(mCg)^2[P_1 P_3 + (P_1 P_3)^* + P_2 P_4^* + P_2^* P_4 + (mCg)^2] = 0,\end{aligned} \tag{A2.1}$$

When mC_g is large, the following expansion for σ is suitable:

$$\sigma = \sigma^{(1)} mC_g + \sigma^{(0)} + \frac{\sigma^{(-1)}}{mC_g} + \ldots \tag{A2.2}$$

When this expansion is substituted into (A2.1) and terms of the same order in mC_g are collected, we obtain the relations

$$(\sigma^{(1)2} + 1)^2 = 0 \tag{A2.3}$$

$$(4\sigma^{(0)} - (P_1 + P_1^* - 2L))(\sigma^{(1)2} + 1)\sigma^{(1)} = 0 \tag{A2.4}$$

$$\begin{aligned}&6\sigma^{(1)2}\sigma^{(0)2} + 2\sigma^{(0)2} - 3(P_1 + P_1^* - 2L)\sigma^{(1)2}\sigma^{(0)} - (P_1 + P_1^* - 2L)\sigma^{(0)} \\ &+[P_1 P_1^* - P_2 P_2^* - 2L(P_1 + P_1^*)]\sigma^{(1)2} + (P_1 P_3 + (P_1 P_3)^* + P_2 P_4^* + P_2^* P_4) \\ &+4\sigma^{(1)}(\sigma^{(1)2} + 1)\sigma^{(-1)} = 0\end{aligned} \tag{A2.5}$$

$\sigma^{(1)}$, solved from the equation (A2.3), is found to be:

$$\sigma^{(1)} = \pm i \tag{A2.6}$$

(A2.4) is satisfied automatically because of (A2.6).

From (A2.5) and (A2.6), $\sigma^{(0)}$ is found to satisfy the quadratic equation:

$$\sigma^{(0)2} - \frac{P_1 + P_1^* - 2L}{2}\sigma^{(0)} - \frac{[P_1 P_3 + (P_1 P_3)^* + P_2 P_4^* + P_2^* P_4] - [P_1 P_1^* - P_2 P_2^* - 2L(P_1 + P_2)]}{4} = 0. \tag{A2.7}$$

References

[1] Akylas, T.R. 1983 J. Fluid Mech. 132, 197-208.

[2] Bowen, A.J. & Inman, D.L. 1969 J. Geophys. Res. 74, 5479-5490.

[3] Galvin, C.J. 1965 Trans. Am. Geophys. Union 46, 112.

[4] Greenspan, H.P. 1956, J. Fluid Mech. 1, 574-592.

[5] Guza, R.T. & Bowen, A.J. 1976 J. Mar. Res. 34, 269-293.

[6] Guza, R.T. & Davis, R.E. 1974 J. Geophys. Res. 79, 1285-1291.

[7] Guza, R.T. & Inman, D.L. 1975 J. Geophys. Res. 80, 2997-3011.

[8] Minzoni, A.A. & Whitham, G.B. 1977 J. Fluid Mech. 79, 273-287.

[9] Stokes, C.G. 1846 In Proc. 16th Meet. Brit. Assn Adv. Sci., Southampton, pp. 1-20. John Murray

[10] Ursell, F. 1952 Proc. Roy. Soc. A 214, 79-97

[11] Whitham, G.B. 1976 J. Fluid Mech. 74, 353-368.